Journal of Inequalities and Applications
a SpringerOpen Journal

RESEARCH Open Access

Multi-resolution wavelet basis for solving steady forced Korteweg–de Vries model

Somlak Utudee[1,2] and Montri Maleewong[3*]

*Correspondence: montri.m@ku.th
[3]Department of Mathematics, Faculty of Science, Kasetsart University, Bangkok, 10900, Thailand
Full list of author information is available at the end of the article

Abstract

A steady forced Korteweg–de Vries (fKdV) model which includes gravity, capillary, and pressure distributions is solved numerically using the wavelet Galerkin method. The anti-derivatives of Daubechies wavelets are developed as the basis of the solution subspaces for the mixed boundary condition type. Accuracy of numerical solutions can be improved by increasing the number of wavelet levels in the multi-resolution analysis. The theoretical result of convergence rate is also shown. The problem can be viewed as gravity-capillary wave flows over an applied pressure distribution. The flow regime can be characterized by subcritical, supercritical, and critical flows depending on the value of the Froude number. Trapped depression and elevation waves are found over the pressure distribution. For a near-critical flow regime, a generalized solitary wave with ripples is presented. This shows a capillary effect in balance to gravity and the pressure force on the free surface.

1 Introduction

Free surface flow is a fundamental problem in fluid dynamics. It has been extensively studied from various points of view. A widely used model is based on weakly nonlinear theory. The Korteweg–de Vries equation in the context of weakly nonlinear analysis has been shown to be a successful model to describe the free surface flows in a transcritical regime. When the free surface interacts with an external forcing, the weakly nonlinear model can be extended and is called a forced Korteweg–de Vries (fKdV) equation. This model can be used in many applications such as for free surface flows past an obstacle or the flows past an applied pressure distribution; see more details in [1, 2].

In view of numerical methods, the fKdV model subjected to initial and boundary conditions can be solved using the finite difference method (FDM), the finite element method (FEM), or the Fourier spectral method (FSM) (see [3–5]). It is usually difficult for FDM to approximate nonlinear term in the form of difference equations. Generally, some suitable bases are needed in approximation spaces. The FEM has an advantage over the FDM, since the nonlinear term and the higher order derivatives can be approximated correctly using some suitable bases. However, in some cases, such as a high gradient wave being interacted with external forcing, very high resolution of mesh points is required to obtain accurate solutions in certain flow regimes. Additionally, the computational time is then

Springer

massive. The adaptive FEM is another choice to resolve the problem, but it requires basic knowledge to define the value of the threshold for setting a new, small element size. Furthermore, its implementation is not easy. The FSM has been successful in solving the fKdV (see [3]) due to its capabilities of handling a nonlinear term accurately. The FSM is accurate and efficient for periodic flow since it applies the Fourier basis in the space of approximation. In fact, the FSM can be used to solve many varieties of non-periodic problems. The key is using a different basis such as the family of orthogonal polynomials, but it is not straightforward to satisfy the cases of mixed or Neumann boundary conditions. Some techniques are required for each specific case. The aim of the current study was to define a suitable basis that can handle nonlinear term and satisfy the boundary conditions with less computational time.

The Galerkin method is a powerful method for solving nonlinear boundary value problems with Neumann, Dirichlet, and mixed boundary conditions, see [6, 7]. There are various types of basis function which can be adopted in the space of approximation. One efficient way is using a wavelet as a basis function, see [8–11]. For instance, the application of Haar wavelets for solving the Schrödinger equation is presented by [12], a delay PDE by [13], or a nonlinear parabolic PDE by [14]. The accuracy of numerical solutions can be improved by increasing just the wavelet level in the multi-resolution analysis. However, development is required of the application of the wavelet basis in the Galerkin method for solving a general type of boundary condition. A suitable wavelet basis must be defined before it can be used to solve each type of boundary conditions (see [15]).

The study of free-surface flows past obstacles or disturbances in a uniform stream has been a much-studied problem over the last three decades, see for instance [16–18]. The disturbances that occur in nature come from various sources of physical situations such as a localized pressure distribution applied on the water wave caused by atmospheric disturbances due to wind force, or a direct perturbation from a moving vehicle on the free surface. When a moving frame of reference with the moving disturbance is considered, localized steady waves in the form of solitary waves are found. The suitable weakly nonlinear model for describing this problem is the fKdV model, see [1] for the problem formulation.

In this work, we develop a wavelet Galerkin method based on the anti-derivatives of Daubechies wavelets (see [15, 19]) which can be applied to solve the fKdV model subjected to mixed boundary conditions. The wavelet basis is designed to satisfy the downstream flow condition. An external forcing is considered as a compact support in the fKdV model. This problem can be viewed as the pressure distribution being applied on the free surface. Gravity and surface tension forces are also included. Furthermore, this problem can be viewed as gravity-capillary wave flows due to an applied pressure distribution that is governed by the fKdV model as shown in equation (1); more details of derivations can be seen in [1]. When the surface tension effect is dominant, ripple waves will be generated on the free surface. These small amplitude waves propagate both upstream and downstream to both endpoints of the flow domain. Dirichlet boundary conditions for wave amplitude are not satisfied. This issue motivates us to develop a suitable basis, such as the wavelet basis, to solve the nonlinear model while satisfying a more general type of boundary conditions at the far fields.

Numerical solutions of the fKdV model can be classified in different flow regimes by subcritical, supercritical, and critical flows depending on the value of the Froude number. We apply the proposed numerical scheme to find various types of steady solutions

corresponding to different values of pressure magnitudes. Aided by our proposed wavelet basis, some new findings in the form of generalized trapped solitary waves are found at some critical values of the Froude number.

The paper is organized as follows. The anti-derivatives of the Daubechies wavelets that form bases for the nested finite-dimensional subspace of the Sobolev space are presented in Sect. 2. The wavelet Galerkin method based on the proposed basis for solving the fKdV model with mixed boundary conditions is developed in Sect. 3. The numerical results are shown in Sect. 4 and our conclusions are in Sect. 5.

2 Anti-derivative wavelet basis

For a closed interval $[a,b]$, let $\mathcal{L}^2(a,b)$ denote the space of square integrable functions on $[a,b]$ with the standard inner product $(\cdot,\cdot)$ defined by

$$(u,v)=\int_a^b u(x)v(x)\,dx$$

with the associated norm $\|\cdot\|$.

Let $\mathcal{H}^s(a,b)$ denote the standard Sobolev space with the norm $\|\cdot\|_s$,

$$\|v\|_s^2=\sum_{i=0}^{s}\int_a^b \left|v^{(i)}(x)\right|^2 dx,$$

where $v^{(i)}$ denotes the i-order derivatives of v and the seminorm $|\cdot|_s$ is defined by

$$|v|_s^2=\int_a^b \left|v^{(s)}\right|^2 dx.$$

It is known that the seminorm $|\cdot|_1$ is a norm in the subspace

$$\mathcal{H}_*^1(a,b):=\left\{v\in\mathcal{H}^1(a,b)|v(a)=0\right\}.$$

We will find a basis for the finite-dimensional subspaces of $\mathcal{H}_*^1(0,L)$ and $\mathcal{H}^1(0,L)$, where $[0,L]$ is the domain of flow problem.

Let $\phi(y)$ be a scaling function and $\psi(y)$ be a wavelet function of order p where p is a positive integer. For $j\geq -1$ and $k\in\mathbb{Z}$,

$$\psi_{j,k}(y)=\begin{cases}\phi(y-k), & j=-1,\\ \sqrt{2^j}\psi(2^j y-k), & j\geq 0,\end{cases}$$

are called the *Daubechies wavelets order p* with support $[0,2p-1]$, see more details in [20, 21]. The set of all wavelets forms an orthonormal basis for $\mathcal{L}^2(\mathbb{R})$, see [15, 19]. We shift the interval $[0,2p-1]$ to $[0,L]$ by the transformation

$$x=\frac{Ly}{2p-1}\in[0,L].$$

Then $\psi_{j,k}$ has the support

$$\left[\left(\frac{k}{2^j}\right)\left(\frac{L}{2p-1}\right),\left(\frac{k+2p-1}{2^j}\right)\left(\frac{L}{2p-1}\right)\right].$$

We define the anti-derivatives of wavelets by

$$\Psi_{j,k}(x) = \int_0^x \psi_{j,k}\, ds \quad \text{for } 0 \le x \le L$$

with the index set D_j by

$$k \in D_j \iff \begin{cases} 2-2p \le k \le 2p-2, & j=-1, \\ 1-p \le k \le 2^j(2p-1)-p, & j \ge 0. \end{cases}$$

In the next theorem we will prove that the set of $\{\Psi_{j,k} | j \ge -1, k \in D_j\}$ is a basis for $\mathcal{H}^1_*(0,L)$. This basis will be used to solve the fKdV model later.

Theorem 2.1 *The set $\{\Psi_{j,k} | j \ge -1, k \in D_j\}$ is a basis for the space $\mathcal{H}^1_*(0,L)$.*

Proof For $j \ge -1$, we define the index set I_j by

$$k \in I_j \iff \begin{cases} 2-2p \le k \le 2p-2, & j=-1, \\ 2-2p \le k \le 2^j(2p-1)-1, & j \ge 0. \end{cases}$$

Let $\operatorname{span}\{\psi_{j,k} | j \ge -1, k \in I_j\}$ be the set of all linear expansions which converge strongly in $\mathcal{L}^2(0,L)$. So $\operatorname{span}\{\psi_{j,k} | j \ge -1, k \in I_j\} = \mathcal{L}^2(0,L)$.

We will show that $\operatorname{span}\{\Psi_{j,k} | j \ge -1, k \in I_j\} = \mathcal{H}^1_*(0,L)$. Since $\Psi'_{j,k} = \psi_{j,k} \in \mathcal{L}^2(0,L)$ and $\Psi_{j,k}(0) = 0$, $\Psi_{j,k} \in \mathcal{H}^1_*(0,L)$. The notation $'$ means the derivative of $\Psi_{j,k}$. Let $u \in \mathcal{H}^1_*(0,L)$. Then its derivative u' is in $\mathcal{L}^2(0,L)$. Since $\operatorname{span}\{\psi_{j,k} | j \ge -1, k \in I_j\} = \mathcal{L}^2(0,L)$, there exist constants $\alpha_{j,k}$ such that

$$\lim_{n\to\infty} \left\| u' - \sum_{j=-1}^{n} \sum_{k\in I_j} \alpha_{j,k}\psi_{j,k} \right\| = 0.$$

Set $u_n = \sum_{j=-1}^{n} \sum_{k\in I_j} \alpha_{j,k}\Psi_{j,k}$. Then $u_n \in \mathcal{H}^1_*(0,L)$ and $u'_n = \sum_{j=-1}^{n} \sum_{k\in I_j} \alpha_{j,k}\psi_{j,k}$. We have

$$|u-u_n|_1 = \|u' - u'_n\| \longrightarrow 0 \quad \text{as } n \longrightarrow \infty.$$

Therefore the linear expansion $\sum_{j=-1}^{\infty} \sum_{k\in I_j} \alpha_{j,k}\Psi_{j,k}$ converges strongly to u in $\mathcal{H}^1_*(0,L)$. Hence, $\operatorname{span}\{\Psi_{j,k} | j \ge -1, k \in I_j\} = \mathcal{H}^1_*(0,L)$. By Proposition 4.2 in [15], the set $\{\psi_{j,k} | -1 \le j \le n, k \in D_j\}$ is a basis for the subspace $\operatorname{span}\{\psi_{j,k} | -1 \le j \le n, k \in I_j\}$. Then the set $\{\Psi_{j,k} | -1 \le j \le n, k \in D_j\}$ is a basis for the subspace $\operatorname{span}\{\Psi_{j,k} | -1 \le j \le n, k \in I_j\}$. It follows that $\{\Psi_{j,k} | j \ge -1, k \in D_j\}$ is a basis for $\mathcal{H}^1_*(0,L)$. □

In multi-resolution analysis, the nested finite-dimensional subspaces S_n of the solution space can be defined by

$$S_n = \operatorname{span}\{\Psi_{j,k} | -1 \le j \le n, k \in D_j\}.$$

By Theorem 2.1, we have that a sequence $\{S_n\}$ is a sequence of finite-dimensional subspaces such that $S_n \subseteq S_{n+1}$ and $\bigcup_{n\in\mathbb{N}} S_n$ is dense in $\mathcal{H}^1_*(0,L)$. We call n the *number of wavelet levels*.

We can apply the Gram–Schmidt process with the standard inner product $(\cdot,\cdot)$ in $\mathcal{L}^2(0,L)$ to obtain an orthonormal basis for $S_n \subseteq \mathcal{H}^1_*(0,L)$, says

$$\{\widehat{\Psi}_{j,k} | -1 \le j \le n, k \in D_j\}.$$

The nested finite-dimensional subspaces of the space $\mathcal{H}^1(0,L)$ can be obtained similarly by setting

$$S_n = \operatorname{span}\{1, \Psi_{j,k} | -1 \le j \le n, k \in D_j\}.$$

Using the Gram–Schmidt process with the standard inner product $(\cdot,\cdot)$ in $\mathcal{L}^2(0,L)$, we obtain an orthonormal basis for $S_n \subseteq \mathcal{H}^1(0,L)$ denoted by

$$\left\{\frac{1}{\sqrt{L}}, \overline{\Psi}_{j,k} | -1 \le j \le n, k \in D_j\right\}.$$

This orthonormal basis will be applied to solve the problem in the next section.

3 Multi-resolution wavelet Galerkin for the forced KdV model

In this section, we use the anti-derivatives of wavelets order p described in the previous section to solve numerically the steady gravity-capillary waves problem which is governed by the forced KdV (fKdV) equation

$$\left(F^2-1\right)u_x - \frac{3}{2}\left(u^2\right)_x + \left(\tau - \frac{1}{3}\right)u_{xxx} = \frac{\epsilon}{2}p_x(x), \tag{1}$$

where u is the free surface elevation, F is the Froude number, τ is the Bond number, ϵ is the magnitude of pressure, and $p(x)$ is the pressure distribution; see more details in [1, 2]. The computational domain is $(0,L)$ with the boundary conditions

$$u(0) = 0, \qquad u'(0) = 0 = u'(L).$$

For the problem, it is assumed that there is a uniform flow with a constant velocity upstream. The values of the Froude numbers $F < 1$, $F = 1$, and $F > 1$ correspond to subcritical, critical, and supercritical flows, respectively. The boundary condition at $x = L$ is given by the Neumann condition which can allow some small amplitude waves downstream. The presented wavelet basis can be used to satisfy these conditions.

The finite dimensional subspace S_n of $\mathcal{H}^1(0,L)$ is employed to solve the fKdV model. Suppose that there exists a weak solution $u \in \mathcal{H}^1(0,L)$. The variation form of (1) can be written as

$$\mathcal{A}(u,v) = \frac{\epsilon}{2}(p_x, v) \quad \text{for all test functions } v \in \mathcal{H}^1(0,L),$$

where

$$\mathcal{A}(u,v) = \left(F^2-1\right)\int_0^L u_x v\,dx - \frac{3}{2}\int_0^L \left(u^2\right)_x v\,dx + \left(\tau - \frac{1}{3}\right)\int_0^L u_{xxx} v\,dx$$

$$(p_x, v) = \int_0^L p_x v\,dx.$$

Let u_n be an approximate solution

$$u_n = \alpha_n \frac{1}{\sqrt{L}} + \sum_{j=-1}^{n}\sum_{k\in D_j} \alpha_{j,k}\overline{\Psi}_{j,k},$$

where α_n and $\alpha_{j,k}$ for $-1 \le j \le n$ and $k \in D_j$ are the unknown wavelet coefficients. Here u_n is the projection of u onto S_n. The variational form can be written by following nonlinear system:

$$\mathcal{A}\left(u_n, \frac{1}{\sqrt{L}}\right) = \frac{\epsilon}{2}\left(p_x, \frac{1}{\sqrt{L}}\right),$$

$$\mathcal{A}(u_n, \overline{\Psi}_{j,k}) = \frac{\epsilon}{2}(p_x, \overline{\Psi}_{j,k}) \quad \text{for all } -1 \le j \le n, k \in D_j.$$

After applying integrating by parts and substituting the boundary conditions $u_n(0) = 0, u_n'(0) = 0 = u_n'(L)$. The nonlinear system for the unknown wavelet coefficients at level n can be solved iteratively by Newton's method. Numerical solutions can be obtained when the values of F, τ, and ϵ are given in the fKdV model.

Next, we will consider the convergence rate of the present scheme. To do this, we prove Lemma 3.1, and the main result is shown in Theorem 3.2.

Lemma 3.1 *For any $u \in \mathcal{H}^{p+1}(0,L)$ and $n \in \mathbb{N}$, there exists a constant $C > 0$ such that*

$$\inf_{v\in S_n} |u-v|_1 \le C\left(2^{-np}\right)|u|_{p+1}.$$

Proof Let $u \in \mathcal{H}^{p+1}(0,L)$. Then its derivative u' is in $\mathcal{L}^2(0,L)$. Since $\{\psi_{j,k} | j \ge -1, k \in D_j\}$ is an orthogonal basis for $\mathcal{L}^2(0,L)$, there exist constants $\alpha_{j,k} = \frac{(u',\psi_{j,k})}{\|\psi_{j,k}\|}$ such that

$$\lim_{n\to\infty}\left\| u' - \sum_{j=-1}^{n}\sum_{k\in D_j}\alpha_{j,k}\psi_{j,k}\right\| = 0.$$

Since $\frac{d}{dx}\left(u - \sum_{j=-1}^{n}\sum_{k\in D_j}\alpha_{j,k}\Psi_{j,k}\right) = u' - \sum_{j=-1}^{n}\sum_{k\in D_j}\alpha_{j,k}\psi_{j,k}$,

$$\lim_{n\to\infty}\left| u - \sum_{j=-1}^{n}\sum_{k\in D_j}\alpha_{j,k}\Psi_{j,k}\right|_1 = 0.$$

Set $u_n = \sum_{j=-1}^{n}\sum_{k\in D_j}\alpha_{j,k}\Psi_{j,k}$. Then $u_n \in S_n$. From the triangle inequality,

$$|u-u_n|_1 = \left|\sum_{j=n+1}^{\infty}\sum_{k\in D_j}\alpha_{j,k}\Psi_{j,k}\right|_1$$

$$\leq \sum_{j=n+1}^{\infty} \left| \sum_{k\in D_j} \alpha_{j,k} \Psi_{j,k} \right|_1 .$$

By the orthogonality of $\{\psi_{j,k} | j \geq -1, k \in D_j\}$, there exists a constant $C_1 > 0$ such that

$$\begin{aligned} \left| \sum_{k\in D_j} \alpha_{j,k} \Psi_{j,k} \right|_1^2 &= \int_0^L \left| \sum_{k\in D_j} \alpha_{j,k} \psi_{j,k} \right|^2 dx \\ &\leq C_1 \left(\sum_{k\in D_j} \alpha_{j,k}^2 \right). \end{aligned}$$

Let $\mathcal{P}_p$ be the space of all polynomials of degree less than p. For any $q(x) \in \mathcal{P}_p$,

$$\begin{aligned} \alpha_{j,k} &= \frac{(u', \psi_{j,k})}{\|\psi_{j,k}\|} \\ &= \frac{1}{\|\psi_{j,k}\|} \int_0^L u' \psi_{j,k} \, dx \\ &= \frac{1}{\|\psi_{j,k}\|} \int_0^L (u' - q) \psi_{j,k} \, dx \\ &\leq \|u' - q\| \quad \text{(Hölder inequality)}. \end{aligned}$$

Note that the length of $\operatorname{supp} \psi_{j,k}$ is $2^{-j}L$. By the Bramble–Hilbert lemma there exists a constant $C_{j,k} > 0$ such that

$$|\alpha_{j,k}| \leq \inf_{q\in\mathcal{P}_p} \|u' - q\| \leq C_{j,k} \left(2^{-j}L\right)^p \left\|u^{(p+1)}\right\| = C_{j,k} \left(2^{-j}L\right)^p |u|_{p+1}.$$

Then

$$\sum_{k\in D_j} \alpha_{j,k}^2 \leq \sum_{k\in D_j} C_{j,k}^2 \left(2^{-j}L\right)^{2p} |u|_{p+1}^2 = C_2 \left(2^{-2jp}\right) |u|_{p+1}^2, \quad \text{where } C_2 = L^{2p} \sum_{k\in D_j} C_{j,k}^2.$$

Therefore

$$\begin{aligned} |u - u_n|_1 &\leq \sum_{j=n+1}^{\infty} \sqrt{C_1 C_2} \left(2^{-jp}\right) |u|_{p+1} \\ &= C \left(2^{-np}\right) |u|_{p+1}, \quad \text{by geometric series, } C = \frac{\sqrt{C_1 C_2}}{2^p - 1}. \end{aligned}$$

□

Theorem 3.2 *Let $u \in \mathcal{H}^{p+1}(0, L)$ and u_n be the projection of u onto the finite-dimensional subspace S_n. Then there exists a positive integer $C > 0$ such that*

$$\|u - u_n\| \leq C \left(2^{-np}\right) |u|_{p+1}. \tag{2}$$

Proof Let $u \in \mathcal{H}^{p+1}(0, L)$. Let u_n be the projection of $u \in \mathcal{H}^1(0, L)$ onto S_n. Then

$$\|u - u_n\| = \inf_{v\in S_n} \|u - v\|.$$

By the Poincaré inequality, there exists $C_1 > 0$ such that $\|w\| \leq C_1|w|_1$ for all $w \in \mathcal{H}^1(0, L)$. Therefore

$$\|u - u_n\| \leq C_1 \inf_{v \in S_n} |u - v|_1.$$

Applying Lemma 3.1, there exists $C_2 > 0$ such that

$$\inf_{v \in S_n} |u - v|_1 \leq C_2\left(2^{-np}\right)|u|_{p+1}.$$

Therefore

$$\|u - u_n\| \leq C\left(2^{-np}\right)|u|_{p+1},$$

where $C = C_1C_2$. □

The main result of Theorem 3.2 is that the rate of convergence is dependent on the wavelet level n and the wavelet order p in the multi-resolution analysis. For example, when $p = 2$, the rate of convergence is approximately 2^{-2} or the error should decrease four times when we increase one wavelet level. In this work we fix $p = 2$ and vary n. Numerical results are obtained when the values of F, τ, and ϵ are given.

4 Numerical results

Before applying the proposed method to solve the fKdV model, we test the accuracy of the numerical scheme by applying it to solve the simple unsteady KdV model with suitable initial and boundary conditions. This has an exact solution in the form of a traveling soliton with constant speed.

4.1 Accuracy test

Consider the unsteady KdV equation

$$u_t + 6uu_x + u_{xxx} = 0, \quad 0 < x < 50, \tag{3}$$

with the boundary and initial conditions

$$\frac{\partial u}{\partial x}(0, t) = 0, \qquad \frac{\partial u}{\partial x}(L, t) = 0, \qquad u(x, 0) = \frac{1}{2}\operatorname{sech}^2\left(\frac{1}{2}\left(x - \frac{L}{2}\right)\right).$$

We apply the present wavelet basis to approximate the solution in space and integrate the solution in time using the fourth order Runge–Kutta method. For each time step, the nonlinear system is solved using Newton's method. To find the wavelet coefficients, a zero solution is set as an initial guess. The wavelet coefficients obtained from the previous time step are set as the initial guess for the next time step. Numerical solution converges within a few iterative steps. All calculations are performed until the final time is reached.

The $x - t$ plot of a traveling solitary wave is shown in Fig. 1. From the initial solitary waveform, this wave moves downstream with constant amplitude. To check the accuracy, the anti-derivative wavelets of order $p = 2$ are applied, while the wavelet level n is varied. The root mean square errors (RMSE) measured at time $t = 20$ for each wavelet level

Figure 1 The $x-t$ plot of traveling solitary wave

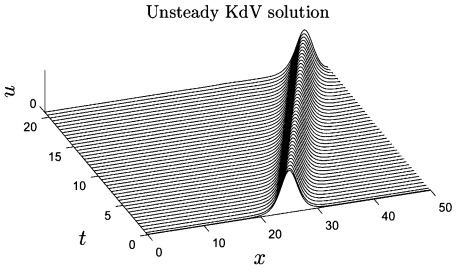

Table 1 Root mean square errors for the unsteady KdV model when $p = 2$ and varied wavelet level n at time $t = 20$

Level	dim	RMSE
4	27	4.1029e-04
5	51	6.4851e-05
6	99	7.3692e-06
7	195	2.7788e-06

Figure 2 The $x-t$ plot of two solitons

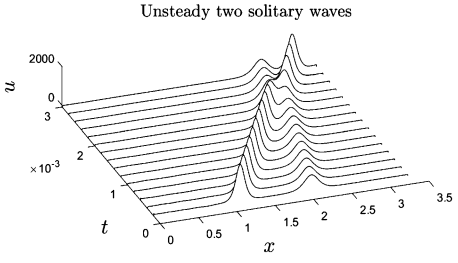

are shown in Table 1. The RMSE decreases when the number of wavelet level increases. The convergence rate is approximately second order, as expected, and it agrees with the theoretical result as shown in Theorem 3.2.

A more complicated initial condition is also investigated. Two solitons are set up initially at time $t = 0$. The initial condition is given by

$$u(x,0) = 3A^2 \operatorname{sech}\big(5\big(A(x+2)\big)\big)^2 + 3B^2 \operatorname{sech}\big(5\big(B(x+1)\big)\big)^2,$$
$$A = 25, B = 16, 0 \le x \le 3.5.$$

These two initial waves are collapsed as time increases. Figure 2 shows the results without oscillation in a solitary wave profile after collapsing. The proposed wavelet basis can handle nonlinear terms in the unsteady KdV model.

4.2 Numerical results for the fKdV equation

In this section, the steady forced KdV equation (1) is solved numerically using the wavelet Galerkin method. The anti-derivative wavelet of order $p = 2$ is used to find all the numerical solutions. The pressure distribution is in a compact support form given by

$$p(x) = \exp\big(\big(-\big(x-(L/2)\big)^2\big)/w\big),$$

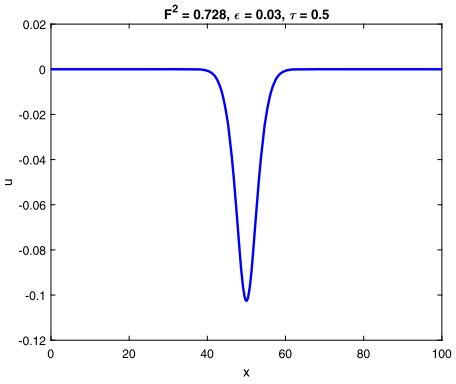

Figure 3 Free surface profile when $F^2 = 0.728$ and $\epsilon = 0.03$

where w and L are the span length and domain range, respectively. Here, we set $w = 20$ and $L = 100$. We restrict our study to the case of a dominated Bond number $\tau = 0.5$, which is greater than the critical value 1/3 from the forced KdV theory, see [1]. This problem can be viewed as a steady flow from upstream (left) to downstream (right) where the uniform flow is specified at the left boundary with a constant incoming flow velocity in terms of the Froude number value. The flow passes the pressure distribution at the middle of the flow domain. The undisturbed free surface level is referenced as $u = 0$. In general, flow regimes can be characterized by the values of the Froude number, where the flow is subcritical when $F < 1$, supercritical when $F > 1$, and critical when $F = 1$. The developed wavelet Galerkin method is applied to find the steady flow solutions in both subcritical and supercritical flow regimes. The Froude number ranges over various values of the pressure magnitude ϵ. The objective is to find a more general type of solitary wave. Numerical results for each flow regime are presented in the following subsections.

4.2.1 Subcritical flow

Consider the case of positive pressure distribution $\epsilon > 0$. For $F^2 = 0.728$ and $\epsilon = 0.03$, the disturbed free surface profile is shown in Fig. 3. The depression wave is trapped over the pressure domain. The wave amplitude $u(0)$ is measured at $x = 50$. The solution branches for various values of $\epsilon > 0$ and $0 < F^2 < 1$ are shown in Fig. 4. As F increases, the depression wave amplitude increases. We cannot find any numerical solutions when F approaches 1. There is a critical value of F for each value of ϵ such that the solution bifurcates to a new branch of the solution (see [1]). The wave amplitude increases very rapidly near the critical value of F. We recover the same type of depression wave as shown in [1].

The type of free surface wave for negative pressure $\epsilon < 0$ is different from that for positive pressure. Solution branches for various values of F and ϵ are shown in Fig. 5. In this case, numerical solutions can be found in the range $0 < F \leq 1$. The solution exists up to the critical value of $F = 1$. The free surface profile of the elevation wave is shown in Fig. 6. The values of the wave amplitude $u(0)$ increases as F increases. This type of trapped elevation wave is bifurcated from uniform flow solutions. The wave amplitude increases when the value of F increases. This type of trapped elevation wave over the pressure distribution is the same as shown in [1].

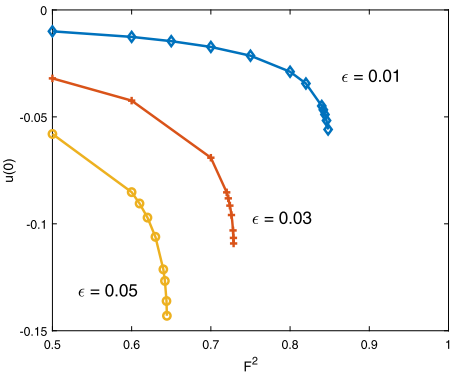

Figure 4 Branch of depression wave for subcritical flows

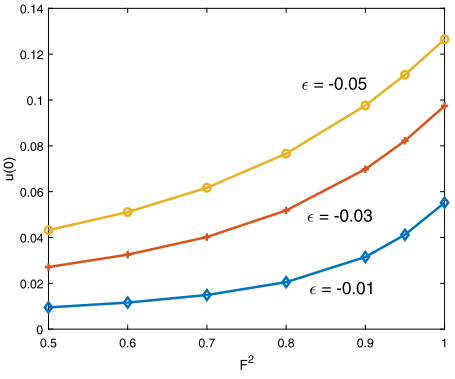

Figure 5 Branch of elevation wave for subcritical flows

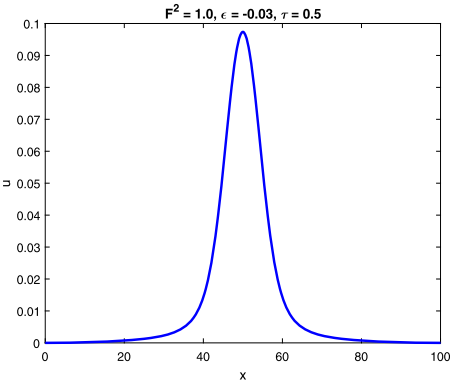

Figure 6 Free surface profile when $F^2 = 1.0$ and $\epsilon = -0.03$

4.2.2 Supercritical flow

The flow is supercritical when $F > 1$. The free surface profile for positive forcing $\epsilon = 0.03$ and $F^2 = 2.8$ is shown in Fig. 7. Wave amplitude is positive over the pressure region. For the same value of ϵ, the elevation wave amplitude increases as F decreases. The case where $F^2 = 1.47$ and $\epsilon = 0.03$ is shown in Fig. 8. The free surface profile is found numerically in the form of the generalized solitary wave which represents the capillary wave effects over the tails of the trapped elevation wave. The capillary effects show many ripples on the free surface. This type of solution occurs near the critical regime when $F > 1$ and $\epsilon > 0$. The solution branches between the wave amplitude and F^2 for various values of $\epsilon > 0$ in the

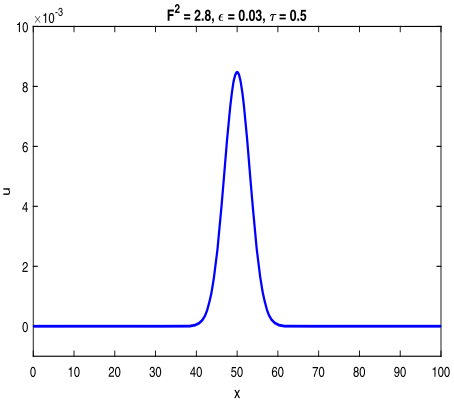

Figure 7 Free surface profile when $F^2 = 2.8$ and $\epsilon = 0.03$

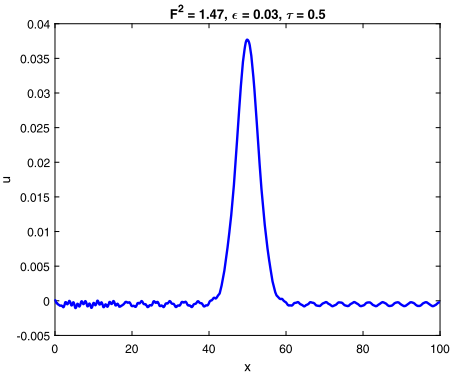

Figure 8 Free surface profile when $F^2 = 1.47$ and $\epsilon = 0.03$

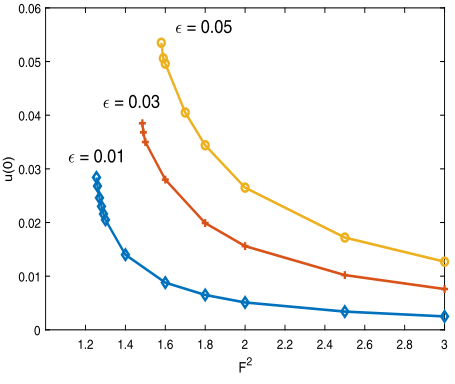

Figure 9 Branch of elevation wave for supercritical flows

case of supercritical flow are shown in Fig. 9. There are critical values of F for each value of ϵ. The mixed boundary condition type at $x = L$ allows us to find this type of the ripple solution. This new result fulfills the solution branch in the bifurcation diagram presented in [1]. Since capillary force is dominated in this case, the ripple appears on the trapped solitary wave.

Similar to the cases involving a trapped elevation wave, trapped depression waves over negative pressure $\epsilon < 0$ are found. The depression wave amplitude increases as F decreases to unity. The solution does not exist for all of the range $F > 1$. There are critical values of F for each $\epsilon < 0$. Trapped depression wave branches for various values of ϵ are shown in

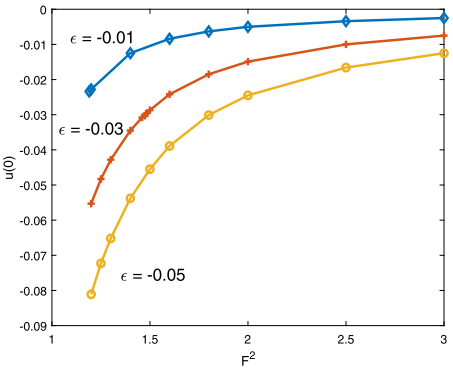

Figure 10 Branch of depression wave for supercritical flows

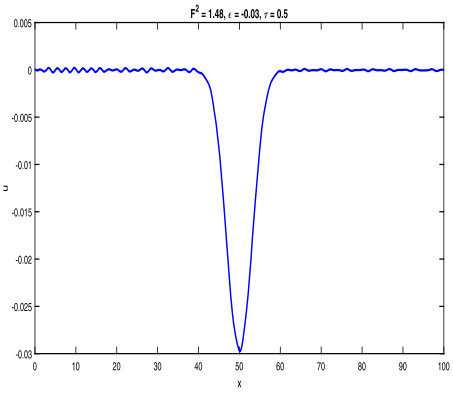

Figure 11 Free surface profile when $F^2 = 1.49$ and $\epsilon = -0.03$

Fig. 10. The free surface profile when $\epsilon = -0.03$ and $F^2 = 1.48$ is shown in Fig. 11. The generalized depression wave with ripples is found when the Froude number approaches a critical value. For $\epsilon = -0.03$, the critical value of F is approximately 1.47. All numerical solutions are bifurcated from the uniform flow solution.

5 Summary and conclusions

Anti-derivative Daubechies wavelets with the Galerkin method are developed in this work. The wavelet basis is designed specifically to solve the mixed-type boundary conditions that cannot usually be applied using a standard wavelet basis space. The proposed numerical scheme is implemented to solve the forced Korteweg–de Vries equation which includes gravity, capillary, and pressure distribution effects. We consider the case of a dominated Bond number $\tau > 1/3$. The flow regimes are characterized by the values of the Froude number. Various types of steady gravity-capillary wave solutions are found. Trapped elevation or depression waves are obtained over the pressure distribution region depending on the sign and the magnitude of the applied pressure. The generalized elevation and depression waves are found near the critical flow regime. These results show capillary effects with ripple waves which are the extended results presented previously in [1]. To obtain this type of solution, the mixed boundary conditions should be applied instead of applying the Dirichlet condition on the far field downstream. The present wavelet basis can handle nonlinear terms in the fKdV model. Further study might apply the numerical scheme to solve the unsteady fKdV with mixed boundary conditions and also investigate the interactions among the gravity, capillary, and forcing effects in each flow regime.

Acknowledgements
This research was supported by Chiang Mai University and the Centre of Excellence in Mathematics, the Commission on Higher Education, Thailand to the first author.

Funding
No funding was received.

Availability of data and materials
Not applicable.

Competing interests
The authors declare that they have no competing interests.

Authors' contributions
All authors contributed equally to this work. All authors have read and approved the final manuscript.

Author details
[1]Advanced Research Center for Computational Simulation (ARCCoS), Department of Mathematics, Faculty of Science, Chiang Mai University, Chiang Mai, 50200, Thailand. [2]Centre of Excellence in Mathematics, CHE, Si Ayutthaya Road, Bangkok, 10400, Thailand. [3]Department of Mathematics, Faculty of Science, Kasetsart University, Bangkok, 10900, Thailand.

Publisher's Note

Received: 21 April 2021 Accepted: 16 September 2021 Published online: 08 October 2021

References

1. Maleewong, M., Asavanant, J., Grimshaw, R.: Free surface flow under gravity and surface tension due to an applied pressure distribution: I Bond number greater than one-third. Theor. Comput. Fluid Dyn. **19**(4), 237–252 (2005)
2. Maleewong, M., Grimshaw, R., Asavanant, J.: Free surface flow under gravity and surface tension due to an applied pressure distribution. II: Bond number less than one-third. Eur. J. Mech. B, Fluids **24**(4), 502–521 (2005)
3. Fornberg, B.: A Practical Guide to Pseudospectral Methods. Cambridge University Press, Cambridge (1996)
4. Jairo Villegas, G., Jorge Castaño, B., Julio Duarte, V., Esper Fierro, Y.: Wavelet–Petrov–Galerkin method for the numerical solution of the KdV equation. Appl. Math. Sci. **6**(69), 3411–3423 (2012)
5. Yu, R.G., Wang, R.H., Zhu, C.G.: A numerical method for solving KdV equation with multilevel B-spline quasi-interpolation. Appl. Anal. **92**(8), 1682–1690 (2013)
6. Amaratunga, K., Williams, J.R.: Wavelet–Galerkin solution of boundary value problems. Arch. Comput. Methods Eng. **4**(3), 243–285 (1997)
7. Choudhury, A.H., Deka, R.K.: Wavelet–Galerkin solutions of one dimensional elliptic problems. Appl. Math. Model. **34**, 1939–1951 (2010)
8. Chen, X., Xiang, J.: Solving diffusion equation using wavelet method. Appl. Math. Comput. **217**, 6426–6432 (2011)
9. Kaur, H., Mittal, R.C., Mishra, V.: Haar wavelet quasilinearization approach for solving nonlinear boundary value problems. Am. J. Comput. Math. **1**(3), 176–182 (2011)
10. Li, B., Chen, X.: Wavelet-based numerical analysis: a review and classification. Finite Elem. Anal. Des. **81**, 14–31 (2014)
11. Liu, X., Zhou, Y., Wang, X., Wang, J.: A wavelet method for solving a class of nonlinear boundary value problems. Commun. Nonlinear Sci. Numer. Simul. **18**(8), 1939–1948 (2013)
12. Pervaiz, N., Aziz, I.: Haar wavelet approximation for the solution of cubic nonlinear Schrödinger equations. Phys. A, Stat. Mech. Appl. **545**, 123738 (2020)
13. Aziz, I., Amin, R.: Numerical solution of a class of delay differential and delay partial differential equations via Haar wavelet. Appl. Math. Model. **40**, 10286–10299 (2016)
14. Saleem, S., Aziz, I., Hussain, M.Z.: A simple algorithm for numerical solution of nonlinear parabolic partial differential equations. Eng. Comput. **36**, 1763–1775 (2020)
15. Xu, J.C., Shann, W.C.: Galerkin–Wavelet methods for two point boundary value problems. Numer. Math. **63**, 123–144 (1992)
16. Dias, F., Vanden-Broeck, J.-M.: Generalised critical free-surface flows. J. Eng. Math. **42**(1), 291–301 (2002)
17. Dias, F., Vanden-Broeck, J.-M.: Trapped waves between submerged obstacles. J. Fluid Mech. **509**, 93–102 (2004)
18. Părău, E., Vanden-Broeck, J.-M.: Nonlinear two- and three-dimensional free surface flows due to moving pressure distributions. Eur. J. Mech. B, Fluids **21**, 643–656 (2002)
19. Utudee, S., Maleewong, M.: Multiresolution wavelet bases with augmentation method for solving singularly perturbed reaction–diffusion Neumann problem. Int. J. Wavelets Multiresolut. Inf. Process. **17**(1), 1850064 (2019). https://doi.org/10.1142/S0219691318500649
20. Daubechies, I.: Ten Lectures on Wavelets. CBMS Series, vol. 61. SIAM, Philadelphia (1992)
21. Hernández, E., Weiss, G.: A First Course on Wavelets. CRC Press, Boca Raton (1996)